

# MICROSCALE THERMAL RELAXATION DURING ACOUSTIC PROPAGATION IN AEROGEL AND OTHER POROUS MEDIA

**John F. T. Conroy, Bouvard Hosticka, Scott C. Davis,  
Andrew N. Smith, and Pamela M. Norris**

*Department of Mechanical and Aerospace Engineering, University of Virginia,  
Charlottesville, Virginia, USA*

*The longitudinal acoustic velocity in silica aerogel is presented as a function of the interstitial gas type and pressure. This was measured using air-coupled ultrasonic transducers configured for differential pulse transit time measurements. The results are interpreted in terms of the thermal relaxation of the acoustic pulse. The microscale temperature oscillations of the gas and solid phases of the aerogel due to the acoustic pulse are not identical if the rate of heat transfer between the two phases is slow compared to the period of the acoustic oscillation. The energy transferred from the gas to the solid phase is lost to the acoustic propagation and, thus, reduces the amplitude and velocity of the acoustic wave. The gas type and pressure may provide independent variables for probing these effects in aerogel.*

Aerogels are highly porous, nanostructured solid media commonly formed by the supercritical drying of a liquid-filled gel. A sol-gel production process involves the hydrolysis and condensation of alkoxy metallates to form a three-dimensional gel. This results in a fractal microstructure composed of nanometer size particles and pores as illustrated in Figure 1. The porosity of aerogels commonly ranges between 85% and 97% and may include micro-, meso-, and macropores. Because of proposed applications as acoustic delay lines, impedance matching layers, and acoustic and thermal insulation, the acoustic properties of aerogels have been the subject of several recent studies [1–6]. The benefits of utilizing aerogels in such applications include an acoustic velocity less than air and an acoustic impedance that is tunable with production conditions.

The theoretical description of acoustic propagation in aerogels is not complete. At ultrasonic frequencies, the porous aerogel microstructure gives rise to unique and anomalous acoustic behavior such as: (1) a nearly linear increase in attenuation with frequency (constant  $Q$ ) in the solid skeleton in the ultrasonic frequency range [4]; (2) a decrease in acoustic velocity with compressive strain [5]; (3) unexplained attenuation bands at distinct ultrasonic frequencies [6]; and (4) a

Received 18 February 1999; accepted 21 April 1999.

This work was sponsored by DARPA under contract MDA972-97-C-0020. The authors would also like to thank Dr. Charles Daitch and Veridian-Pacific Sierra Research for their support.

Address correspondence to Prof. Pamela M. Norris, Department of Mechanical and Aerospace Engineering, Thornton Hall, University of Virginia, Charlottesville, VA 22903, USA. E-mail: pamela@virginia.edu

## NOMENCLATURE

<p><math>A</math> amplitude of sinusoidal temperature variation</p> <p><math>c</math> compressional wave speed</p> <p><math>C</math> specific heat</p> <p><math>C_v</math> specific heat at constant volume</p> <p><math>C_p</math> specific heat at constant pressure</p> <p><math>E(T)</math> average energy of the phase</p> <p><math>f</math> volume fraction</p> <p><math>k</math> wave vector of the acoustic pulse and temperature oscillations</p> <p><math>k_1</math> real component of wavevector <math>k</math></p> <p><math>k_2</math> imaginary component of wave vector <math>k</math></p> <p><math>M</math> molecular weight</p> <p><math>P</math> gas pressure</p> <p><math>Q</math> thermal energy</p> <p><math>t</math> time</p> <p><math>\Delta t</math> difference in time of flight with and without the aerogel</p>	<p><math>T</math> temperature</p> <p><math>x</math> thickness</p> <p><math>\alpha</math> attenuation per wavelength</p> <p><math>\beta</math> bulk modulus</p> <p><math>\gamma</math> ratio of specific heats</p> <p><math>\rho</math> density</p> <p><math>\tau</math> relaxation time</p> <p><math>\omega</math> frequency of acoustic pulse and temperature oscillations</p> <p style="text-align: center;"><b>Subscripts</b></p> <p>Eq equilibrium</p> <p><math>G</math> gas phase</p> <p><math>O</math> initial</p> <p><math>S</math> solid phase</p> <p><math>T</math> isothermal</p>
-------------------------------------------------------------------------------------------------------------------------------------------------------------------------------------------------------------------------------------------------------------------------------------------------------------------------------------------------------------------------------------------------------------------------------------------------------------------------------------------------------------------------------------------------------------------------------------------------------------------------------------------------------------------------------------------------------------------------------------------------------------------------------------------------------------------------------------------	---------------------------------------------------------------------------------------------------------------------------------------------------------------------------------------------------------------------------------------------------------------------------------------------------------------------------------------------------------------------------------------------------------------------------------------------------------------------------------------------------------------------------------------------------------------------------------------------

decrease in attenuation by the solid skeleton with increasing temperature [4]. The following investigation was undertaken in order to further elucidate the acoustic and microstructural behavior of aerogels and other highly porous media.

To date, the theoretical interpretation of acoustic propagation at ultrasonic frequencies in aerogels has been limited to a form of the classical Wood equation [7]. This approach considers both components of a composite medium to be contributing independently to the overall properties of an elementary volume with the same average properties as the bulk. Thus, the density of the elementary volume is the volume fraction weighted average of the densities of the two (or more) independent components. Likewise, the bulk modulus of the elementary volume is the volume fraction weighted average of the bulk moduli of the two (or more) independent components. The Wood equation predicts a compressional

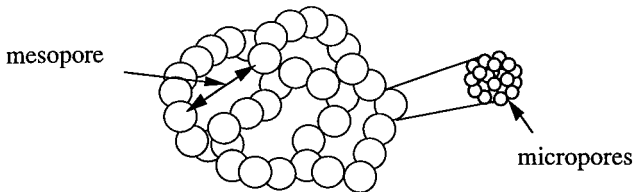


**Figure 1.** Conceptual portrayal of the aerogel microstructure. Mesopore dimensions are tens to hundreds of nanometers; micropore dimensions are a few nanometers. In the aerogel sample examined in this study at STP, there are approximately 100 gas molecules per mesopore and the mean mesopore diameter is smaller than the mean free path of the ambient gas.

wave speed,  $c$ , of

$$c = \left[ (f_S \rho_S + f_G \rho_G) \left( \frac{f_S}{\beta_S} + \frac{f_G}{\beta_G} \right) \right]^{-1/2} \quad (1)$$

where  $f_S$ ,  $f_G$ ,  $\rho_S$ ,  $\rho_G$ ,  $\beta_S$ , and  $\beta_G$  represent the respective volume fraction, density, and bulk modulus of the solid and gas, respectively. A modified version of this equation has been shown to be effective for describing the observed dependence of acoustic velocity on pressure of the interstitial gas in extremely low-density aerogels ( $< 50 \text{ kg/m}^3$ ) in pressures ranging between atmospheric and vacuum [2]. However, the Wood approach has been shown by other researchers to be inaccurate when the skeletal backbone is solid [8, 9].

Other traditional methods for describing acoustic propagation in fluid-filled porous media are poorly adaptable to aerogels. For example, Biot theory [10, 11] and the dynamic tortuosity approach of Johnson et al. [12] are continuum approaches that describe the coupling of the two component phases through viscous and thermal characteristic lengths based on the continuum viscosity and thermal conductivity of the fluid phase. The continuum assumption is not applicable to aerogel, where the thermal conductivity [13] and gas flow [14] have already been shown to be molecular rather than bulk phenomena at ambient pressures. In this regime, the microscopic thermal transport processes of the gas cannot be described by a continuum temperature profile or thermal boundary layer. To the best of our knowledge, there has been no extension of these traditional methods to the microscale regime, where the continuum assumption is no longer applicable.

This article provides a novel theoretical basis for examining microscale thermal effects during acoustic propagation in gas-filled aerogels. As other researchers have indicated [2], acoustic transmission in the gas inside an aerogel is likely to be more isothermal than in the pure gas, because of the intimate contact between the gas and the solid phases. This article considers the nature of the microscale thermalization of the two component phases and the influence of these microscale effects on the bulk acoustic properties of aerogel. Specifically, thermal relaxation effects will be described that are due to heat exchange between two component phases and give rise to a dynamic heat capacity and bulk modulus of the interstitial gas. The mathematics of this approach closely follow classical thermal relaxation due to heat exchange between states, as in polyatomic gases and gaseous mixtures [15].

## BACKGROUND

The aerogels used in this study are made from silica and have a porosity of approximately 97% and a density of approximately  $70 \text{ kg/m}^3$ . A mean mesopore diameter of 20 nm has been determined using nitrogen sorption porosimetry. This mesoporosity accounts for approximately 33% of the total porosity in the aerogel. Given the production conditions and optical clarity of these aerogels [16], the majority of the remaining porosity is expected to have pore diameters smaller than 10 nm.

Interstitial atmospheric gases at STP in these nanoporous materials are more likely to collide with the solid pore wall than with other gas molecules. For example, the mean free path of nitrogen at STP is approximately 85 nm, which yields a Knudsen number of greater than 4 in the mesopore regime. Furthermore, the molecular volume (volume per molecule gas) of a gas at STP is  $3.7 \times 10^{-26} \text{ m}^3$ . This is approximately 1/100th of the volume of the average mesopore. The conceptual model for describing the gas dynamics inside a mesopore should bear a closer relationship to ultrahigh vacuum (UHV) systems than those typically used to describe porous media.

The microscopic response to acoustic propagation in a gas and a solid is very different. In a pure ideal gas, nearly adiabatic heating and cooling accompany the successive compression and rarefaction of an acoustic pulse. Under typical conditions, the temperature swings are of the order of 0.01 K. However, the temperature swings in a solid are much smaller, reflecting the lower adiabatic compressibility. Within an aerogel, this heterogeneity in the thermal response results in temperature gradients on the size scale of the pore diameter.

The heat transfer between components resulting from these microscale temperature gradients will have an impact upon the bulk acoustic behavior of aerogel. The process can be likened to thermal relaxation in polyatomic gases and mixtures of gases [13, 17]. The solid component of the aerogel is analogous to the nontranslational states of a polyatomic gas, while the gaseous component is analogous to the translational states. The energy transferred from the gaseous component to the solid component is lost to the acoustic propagation in the gaseous component, much as the energy transferred out of the translational states is lost. This results in an increased absorption of the acoustic pulse and a decreased acoustic velocity.

## THERMAL RELAXATION IN A TWO COMPONENT SYSTEM

The conceptual model of thermal relaxation on which this derivation is based is shown in Figure 2. The aerogel is divided into a series of volume elements that are small relative to the wavelength of the acoustic pulse and have an open porosity identical to the net porosity of the entire aerogel. Two thermodynamically distinct components exist within each volume element, namely, a solid phase  $S$  and a gas phase  $G$ . The solid phase is assumed to be arbitrarily shaped, with an average pore diameter as given by nitrogen sorption measurements.

The total energy of this system,  $E(T)$ , is distributed between both the solid and gaseous phases. Since the two component phases are thermodynamically distinct, they each have a separate temperature,  $T_S$  and  $T_G$ , molar specific heat at constant volume,  $C_S$  and  $C_{vG}$ , and average internal energy,  $E_S(T_S)$  and  $E_G(T_G)$ . It is thus assumed that the internal energy of the solid phase  $E_S$  is independent of the pressure of the gas phase  $P$ . When the temperature of one of the components (or a fraction of the component) is suddenly increased, some amount of redistribution of energy must occur. This redistribution will occur both within other portions of the same component and with the other component phase. During acoustic propagation, the average local temperature of the gaseous component will be subject to much larger fluctuations than the solid component. The redistribution of

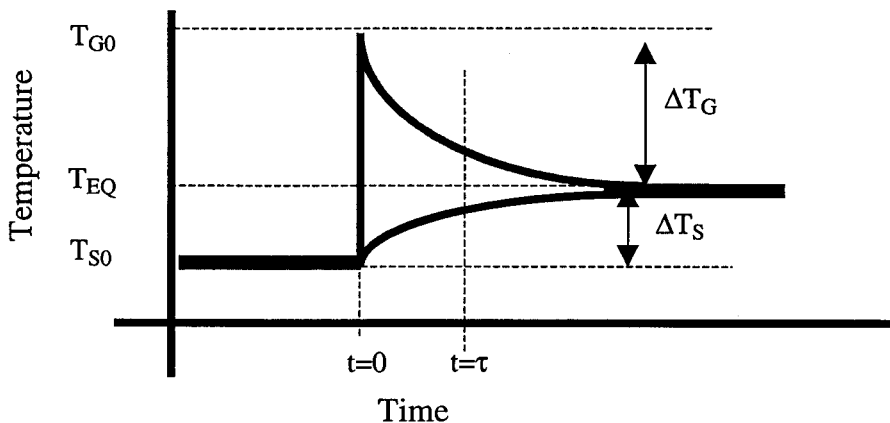


**Figure 2.** Exponential relaxation of the temperature heterogeneity inside the aerogel. A sudden input of energy into the gas will be followed by the thermalization of the two component phases of the aerogel. In the analysis presented here, the temperature of the solid component is not fixed. The relaxation time is an empirical relationship that includes the specific heat of both components and the heat transfer coefficient between the two components.

the local gaseous temperature fluctuations will occur with both the neighboring gas molecules and with the solid component. Given the high Knudsen number, this redistribution is a microscale phenomenon. The rate of redistribution will be a function of the heat transfer coefficient between the gas and the solid component.

Starting with the formalism derived by Herzfeld for a mixture of two gases [13] and adapting it to the unique circumstances of a solid matrix component, one has:

- $\tau_S$ , the relaxation time of component  $S$  with itself
- $\tau_G$ , the relaxation time of component  $G$  with itself
- $\tau_{SG}$ , the relaxation time of component  $S$  with  $G$
- $\tau_{GS}$ , the relaxation time of component  $G$  with  $S$

The relaxation times of the solid phase with itself,  $\tau_S$ , and of the solid with the gas,  $\tau_{SG}$ , should have a negligible influence on the acoustic velocity in the solid component. The temperature oscillations are too small to cause a significant change in either the modulus or density of the solid and can be neglected. The relaxation time of the gas with itself,  $\tau_G$ , is the classical Kirchoff (thermal conductivity) relaxation time [18]. The Kirchoff relaxation time,  $\tau_G$ , which is on the order of  $10^{-10}$  seconds at STP for most pure gases, should be decreased in the aerogel due to the low conductivity of both the gas [14] and solid [13] phases. This will increase the frequency at which these effects become significant. Although Kirchoff relaxation is neglected here, it can be readily incorporated at a later point [15]. The remaining relaxation time,  $\tau_{GS}$ , accounts for the relaxation of the gas  $G$  with the solid component  $S$ .

The physical interpretation of  $\tau_{GS}$  is the time constant for heat exchange between the gas phase  $G$  and the solid phase  $S$  as the gas molecules collide with the solid matrix component. Heat exchange between gases and solids has been considered in depth for several years [19–22]. The relaxation time of the gas with the solid,  $\tau_{GS}$ , should reflect (1) transport of individual gas molecules to the solid surface, (2) the energy imparted upon collision with the surface, and (3) energy imparted during contact with the surface. In classical gas dynamic terms, these contributions are defined through the frequency of collision, the heat capacity of the gas and solid, the energy transferred per collision, and the amount of trapping of the gas by the surface, typically grouped as an accommodation coefficient. Experimentally, these parameters can be accessed using different gases at different pressures and temperatures, and different aerogels with different pore sizes and microstructures.

Assuming that the temperature variations are small enough such that specific heat is constant, then the rate of change of the average temperature of the gas phase can be expressed as

$$\frac{dT_G}{dt} = \frac{T_S - T_G}{\tau_{GS}} \quad (2)$$

where the relaxation time  $\tau_{GS}$  is determined by the heat transfer coefficient between the gas and the solid and the specific heat of the two phases.

Figure 2 assumes an exponential thermalization of the average temperatures of the gas phase  $T_G$  and solid phase  $T_S$  to an equilibrium temperature  $T_{Eq}$ . Equation (2) can be modified to include the equilibrium temperature,  $T_{Eq}$ , and an energy balance can be used to find

$$\frac{d(T_G - T_{Eq})}{dt} = \frac{T_S - T_G}{\tau_{GS}} \quad (3)$$

and

$$C_{vG}T_G + C_S T_S = (C_{vG} + C_S)T_{Eq} \quad (4)$$

Combining Eqs. (3) and (4) to solve for the temperature of the gas,  $T_G$ , and integrating yields

$$T_G - T_{Eq} = (T_G - T_{Eq})_{t=0} \exp\left(-\frac{t}{\tau_{GS}} \frac{C_G + C_S}{C_S}\right) \quad (5)$$

In describing the energy change of the gas phase  $G$  due to the acoustic pulse, the standard thermodynamic identity can be modified to give [15]

$$\frac{dQ_G}{dt} = \left(C_{vG} + C_S \frac{\partial T_S}{\partial T_G}\right) \frac{\partial T_G}{\partial t} - T_G \left(\frac{\partial P}{\partial T_G}\right)_{v, \rho_0 G} \frac{M_G}{\rho_0 G} \frac{\partial \rho_G}{\partial t} \quad (6)$$

where  $Q_G$  is the thermal energy of the gas,  $M_G$  is the molar mass of the gas,  $\rho_G$  is the density of the gas, and  $\rho_{0G}$  is the initial density of the gas. The thermal energy described in the second term on the right-hand side accounts for the temperature variations due to the change in pressure caused by the acoustic wave itself. The first term encompasses both the specific heat of the gas and the specific heat due to thermal relaxation with the solid matrix component. The apparent specific heat of the gas is increased with the addition of the solid matrix component by a factor of  $C_S(\partial T_S/\partial T_G)$ , which corresponds to the ratio of heat transferred between the two component phases.

If a sinusoidal variation in the average temperature  $T_S$  and  $T_G$  of amplitude  $A_S$  and  $A_G$  of the solid phase and gas phase due to the propagation of the longitudinal wave is assumed, then

$$T_G = A_G e^{j\omega t + \phi} + T_0 \quad (7)$$

and

$$\frac{dT_S}{dt} = A_S j\omega e^{j\omega t + \phi} = j\omega(T_S - T_0) \quad (8)$$

Combining with Eq. (2), we have

$$\frac{dT_S}{dT_G} = \frac{1}{1 + j\omega\tau_{GS}} \quad (9)$$

Thus, in the limit as  $\omega\tau_{GS}$  goes to infinity, the influence of the solid phase on the apparent heat capacity and relaxation in the gas disappears, and the system should return to the state of the pure gas.

The dispersion relation in the gas is thus similar to that obtained with polyatomic gases [17], and is given by

$$k^2 = \frac{\rho_{0G} \omega^2}{\beta_{TG}} \frac{C_{vG} + C_S(1 + j\omega\tau_{GS})^{-1}}{C_{pG} + C_S(1 + j\omega\tau_{GS})^{-1}} \quad (10)$$

where  $\beta_{TG}$  is the isothermal bulk modulus of the gas and  $C_{pG}$  is the specific heat at constant pressure of the gas. The specific heat at constant pressure of the gas  $C_{pG}$  arises due to modification of the adiabatic equation of state of the ideal gas, given later in Eq. (17).

This approach can be used to account for the influence on the gas of heat exchange with the solid component. It is assumed that the acoustic properties of the solid remain unchanged by the temperature fluctuations, since the changes in density and modulus with temperature of the solid are small. Furthermore, the dispersion relation given in Eq. (10) can be incorporated into a more complete analysis of the porous medium as a whole. This would allow for consideration of density, modulus, and thermal effects on acoustic propagation in aerogel and other nanoporous media.

Although a more complete description of the acoustic propagation in aerogel is being developed for integration with this type of thermal relaxation approach, one can readily return to the elementary volume Wood equation. The Wood equation modified with the complex bulk modulus of the gas then becomes

$$k^2 = \omega^2(f_S \rho_S + f_G \rho_{0G}) \times \left( \frac{f_S}{\beta_S} + \frac{f_G}{\beta_{TG} \left\{ [C_{pG} + C_S(1 + j\omega\tau_{GS})^{-1}] / [C_{vG} + C_S(1 + j\omega\tau_{GS})^{-1}] \right\}} \right) \quad (11)$$

While this expression encompasses the density, modulus, and thermal effects of the porous aerogel medium, it retains the inconsistencies with regards to the solid skeleton mentioned earlier. Although it is probably not a definitive description of acoustic propagation in aerogel, such an expression might clarify some of the previously observed anomalies. For example, the attenuation bands described by Gibiat et al. [6] are accounted for in this model. Allowing the wavevector  $k$  to take complex values to account for attenuation, as in

$$k = k_1 - k_2 j \quad (12)$$

the attenuation per wavelength  $\alpha$  is given by

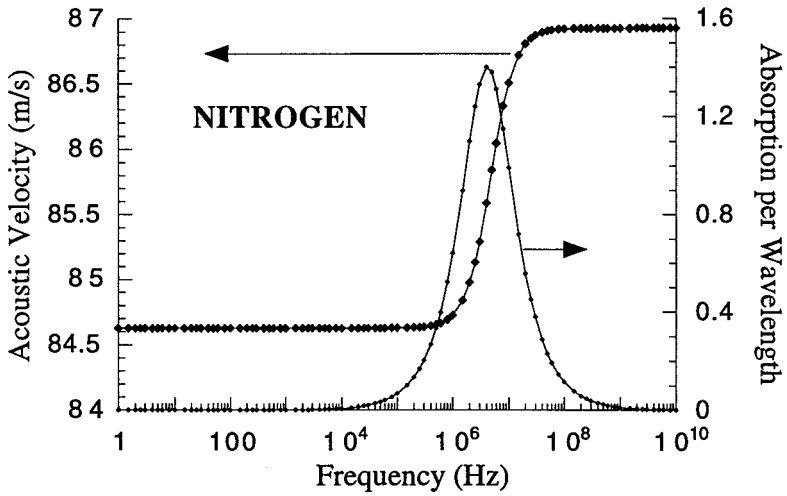
$$\alpha = 2\pi \frac{k_2}{k_1} = -\pi c^2 \frac{f_G}{\beta_{TG}} (f_S \rho_S + f_G \rho_{0G}) \frac{\omega \tau_{GS} C_S (C_{vG} - C_{pG})}{(C_{pG} + C_S)^2 + C_{pG}^2 \omega^2 \tau_{GS}^2} \quad (13)$$

Figures 3a–3c give acoustic velocity and attenuation per wavelength for each gas as a function of frequency in a 71-kg/m<sup>3</sup> aerogel at STP assuming a relaxation time  $\tau_{GS}$  of 0.1  $\mu$ s and a solid bulk modulus of 400 kPa. The values were calculated using Eqs. (11) and (13) and neglected other thermal relaxation mechanisms in the gas phase, such as Kirchhoff relaxation. The dispersion introduced by the complex bulk modulus of the gas results in a total change in compressional acoustic velocity of between 2 and 50 m/s and a local peak in absorption per wavelength. This local peak in absorption may be responsible for the previously observed attenuation bands, and may provide a convenient noncontact method for probing the aerogel microstructure.

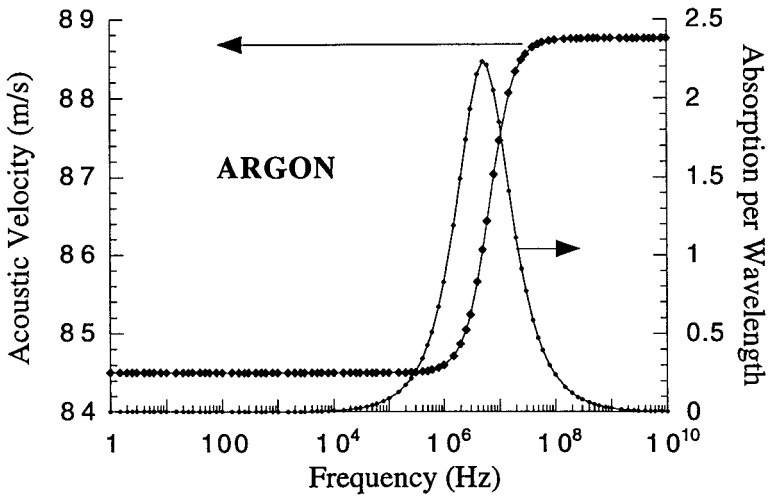
## EXPERIMENTAL

The relaxation time  $\tau_{GS}$  is the exponential time constant for microscale thermalization of the entire gaseous component with the solid component. The relaxation time includes the heat transfer coefficient as well as the specific heats of the two components. The heat transfer coefficient should include the distribution of collisional frequencies within the geometry of an elementary volume, as well as other terms which contribute to an accommodation coefficient, such as the energy



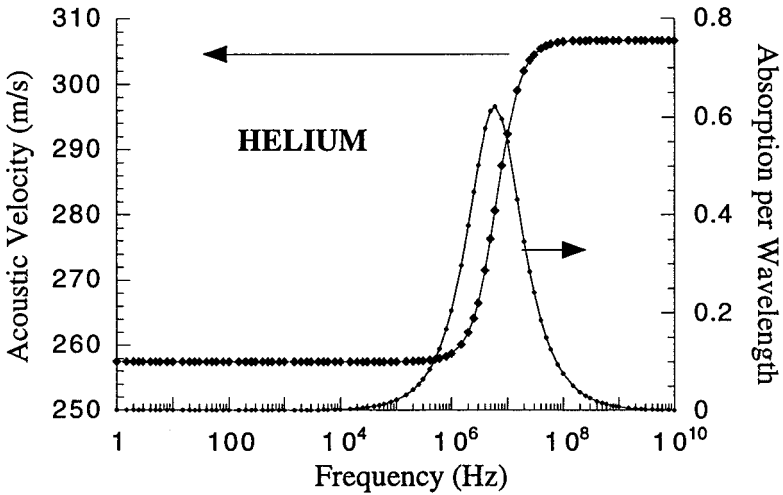


(a)



(b)

**Figure 3.** Acoustic velocity and attenuation per wavelength calculated from Eqs. (11) and (13) for (a) nitrogen, (b) argon.



(c)

**Figure 3.** Acoustic velocity and attenuation per wavelength calculated from Eqs. (11) and (13) for (c) helium assuming a relaxation time of  $0.1 \mu\text{s}$ , an aerogel density of  $0.071 \text{ g/ml}$ , and a solid component bulk modulus of  $400 \text{ kPa}$ . The previously observed attenuation bands at ultrasonic frequencies may be accounted for by the thermalization of the solid and gaseous component of the aerogel. There is no attempt to include Kirchhoff relaxation in any of the plots or internal-external energy conversion in diatomic nitrogen.

transferred per collision and the amount of trapping on the surface. Isolating the individual contributions of these different physical properties is a goal of the experimental portion of this research.

One can begin to isolate the contributions of these various parameters by varying the pressure of different interstitial gases within a variety of aerogels. The heat transferred per collision, as well as the trapping on the surface, should remain constant for a given gas and solid at a given temperature. By changing gases and the microstructure of the solid component, one can probe the collisional frequency, the energy transferred upon collision, and the heat transferred during contact or trapping.

The experimental apparatus is fully described by Conroy et al. [23]. Briefly, the longitudinal acoustic velocity in aerogel samples was calculated as a function of pressure for several gases using a noncontact, differential pulse transit time method. Experiments were performed using a pair of 215-kHz air-coupled transducers (International Transducer Corporation, Santa Barbara, CA) to avoid strain variability and difficulty in obtaining sufficient acoustic coupling. These transducers have a center frequency of 215 kHz with a bandwidth of 30 kHz and a beam angle of  $10^\circ$ .

The aerogel itself was mounted to a motor-driven translation stage that positioned the aerogel in and out of the primary path of the acoustic pulse. The acoustic velocity inside the aerogel  $c$  of thickness  $x$  was calculated using the simultaneously measured acoustic velocity in the pure gas  $c_G$  and the difference in

arrival time  $\Delta t$  with and without the aerogel present, as in

$$c = \frac{x}{\Delta t + x/c_G} \quad (14)$$

A Panametrics 5550 pulser/receiver was used to both drive the transmitter and amplify the received signal of both transducers. The additional delay in the arrival time of the initial pulse introduced by the aerogel was measured with a LeCroy 9324 oscilloscope. The arrival time in these experiments was defined as the point when the amplitude of the initial pulse was equal to twice the noise level.

The transducer assembly was mounted and sealed inside a pressure vessel. To establish a concentration of less than 0.05% air in the test gas, several vessel pressurization–depressurization cycles were performed. A final pressurization stage raised the pressure inside the vessel to 11,000 kPa, and data were collected during the subsequent depressurization. A heated bath was used to maintain a gas temperature of  $300 \pm 0.3$  K. Insertion losses at the air/aerogel interface and hence experimental uncertainty increased with decreasing pressure, as the interstitial gas density was a significant contribution to the total aerogel density.

Silica gels were prepared using a two-step, acid–base-catalyzed hydrolysis / condensation reaction. A catalyst solution (110 ml deionized water, 50 ml 200-proof ethanol, 0.5 ml 30% aqueous ammonium hydroxide) was slowly mixed with a prehydrolyzed silica solution (70 ml ethanol, 70 ml Silbond H-5, Silbond Corp., Weston, MI). Prior to gelation, this mixture was cast into 150-mm-diameter by 6-mm-thick disks. Solvent exchanges to replace the initial reactants with pure ethanol and subsequently ethanol with liquid carbon dioxide were performed prior to supercritical drying. The dried samples were not sintered or otherwise treated prior to investigation. Nitrogen sorption isotherms and the adsorption pore size distribution were determined with a Micrometrics Pore Size Analyzer. The average mesopore apparent diameter was 24 nm, with a standard deviation of 1 nm over five samples. The density of the particular sample examined here was  $71 \text{ kg/m}^3$ .

Figure 4 shows the acoustic velocity through an aerogel as a function of nitrogen, helium, and argon pressure. The acoustic velocity through the aerogel approaches 110 m/s for all three gases at pressures near ambient. This corresponds well with previously reported values for silica aerogels of similar density [2]. The rate of increase of acoustic velocity with increasing pressure is greatest in the gases with the largest acoustic velocity of the free gas.

## DISCUSSION

Three different variants of the Wood equation are used in Figures 5a–5c to analyze the influence of heat exchange on each of the examined gases. All three variants are solved for the acoustic velocity through the aerogel with a constant bulk modulus of the solid component  $\beta_S$  but different bulk moduli of the gas  $\beta_G$ . In the physical system, the bulk modulus of the solid component  $\beta_S$  should be unchanged by the pressure of the interstitial gas (assuming an open pore structure), and was assigned a value of 400 kPa for the purposes of these calculations. Ideal gas behavior and a solid silica specific heat of  $44.77 \text{ J/K mol}$  were also assumed.

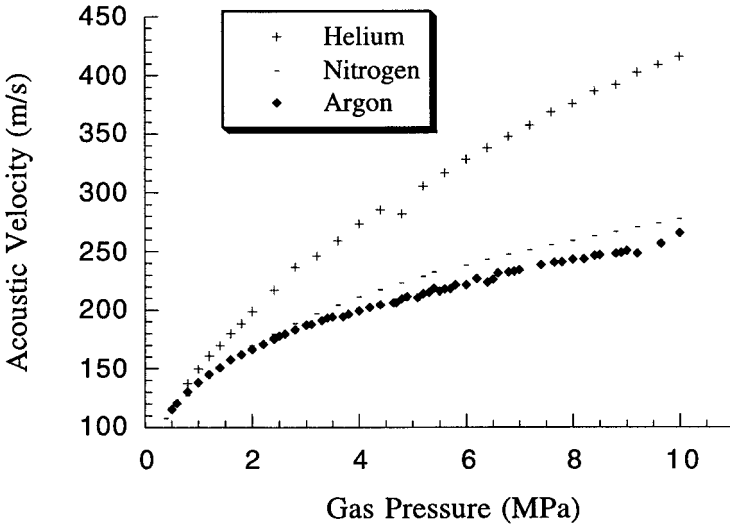


**Figure 4.** Acoustic velocity in the aerogel as a function of pressure of the interstitial gas. The acoustic velocity was measured with air-coupled transducers at 215 kHz using a differential pulse transit time method. The rate of increase of acoustic velocity with pressure is greatest in the gases with the greatest acoustic velocity of the free gas.

The first variant of the gas bulk modulus  $\beta_G$  has been previously examined by Gross et al. [2] and assumes an independent isothermal gas compression with no heating of the solid component, or

$$\frac{P}{P_0} = \frac{\rho_G}{\rho_{0G}} \quad (15)$$

and

$$\beta_G = \beta_{TG} = \rho_{0G} \frac{dP}{d\rho_G} = P_{0G} \quad (16)$$

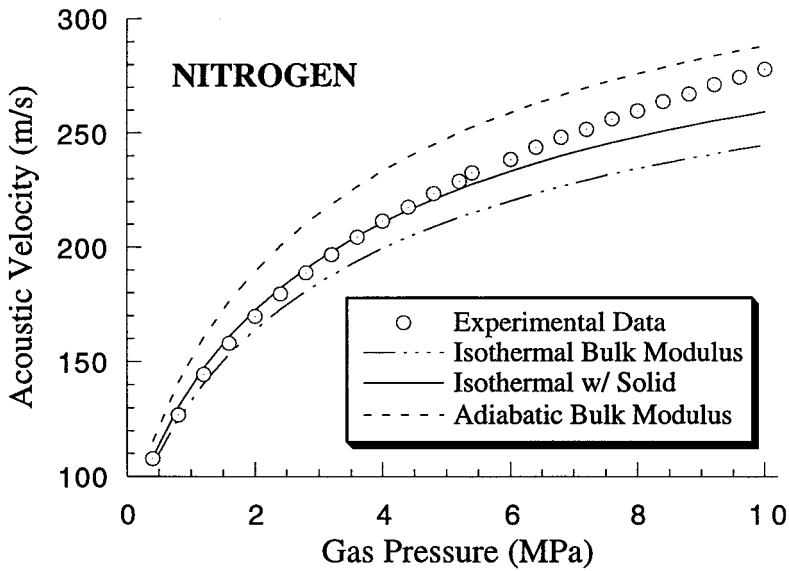
The second variant assumes a standard, completely adiabatic compression, or

$$\frac{P}{P_0} = \left( \frac{\rho_G}{\rho_{0G}} \right)^\gamma \quad (17)$$

and

$$\beta_G = \gamma \beta_{TG} = \gamma P_0 \quad (18)$$

where  $\gamma$  is the ratio of specific heats. The adiabatic bulk modulus of the gas can also be obtained from Eq. (11) when the relaxation time or the frequency of the acoustic propagation is infinite. This corresponds to the limiting case of no heat exchange between the two components.



(a)

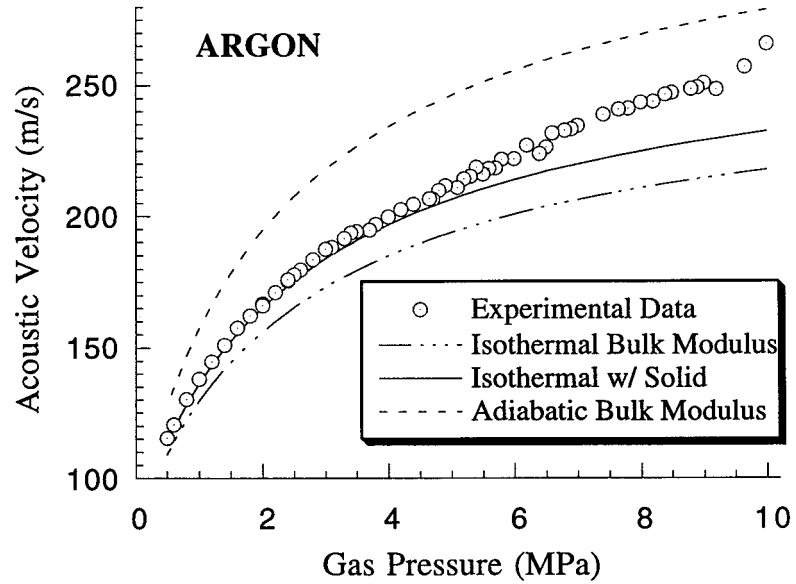
**Figure 5.** Derived acoustic velocity for the aerogel based on the Wood equation using three different expressions for the gas bulk modulus. (a) Nitrogen.

The third and final variant is the isothermal form of Eq. (11), where heat exchange between the two component phases occurs instantaneously or the oscillation frequency goes to infinity, and the temperature of both phases change synchronously. The bulk modulus of the gas  $\beta_G$  then becomes

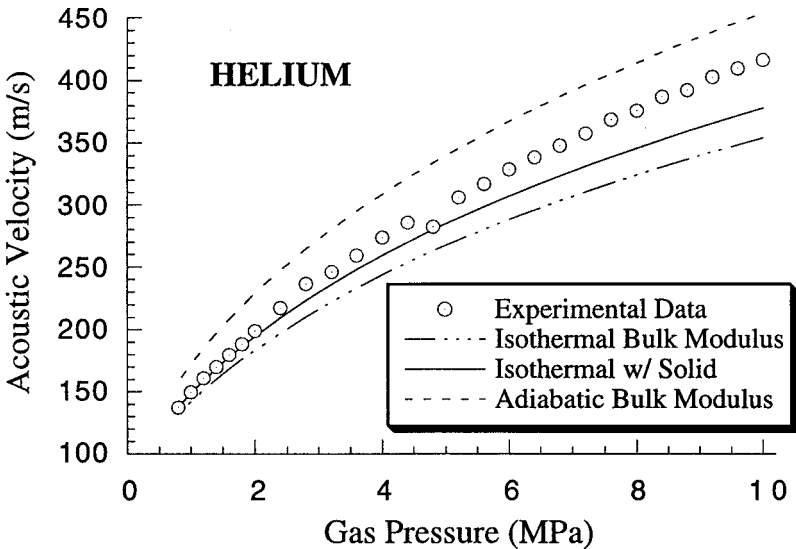
$$\beta_G = \beta_{TG} \frac{C_{pG} + C_S}{C_{vG} + C_S} = P_0 \frac{C_{pG} + C_S}{C_{vG} + C_S} \tag{19}$$

As shown in Figures 5a–5c for the three gases, the two forms of isothermal gas bulk moduli consistently underpredict the acoustic velocity, while the adiabatic gas bulk modulus consistently overpredicts the measured velocity. This can be taken as an indication of mixed isothermal and adiabatic acoustic propagation in the gas arising due to aerogel nanostructure. Since the other parameters can be measured independently, the acoustic propagation in the aerogel can be described using the Wood equation only through combined adiabatic and isothermal character of the propagation in the gas.

By using a curve fit of the measured acoustic velocity data, the relaxation times  $\tau_{GS}$  as in Eq. (11) can be calculated for each gas. Thus, the bulk modulus of



(b)



(c)

**Figure 5.** Derived acoustic velocity for the aerogel based on the Wood equation using three different expressions for the gas bulk modulus. (b) argon, and (c) helium are the gases. A correct gas bulk modulus should predict the acoustic velocity at each pressure accurately. However, the isothermal models consistently underpredict acoustic velocity, while the adiabatic model overpredicts acoustic velocity. A complex bulk modulus and heat capacity as described in the text can be used to account for the combined adiabatic and isothermal nature of the gas-phase compression during acoustic propagation in the aerogel.

the gas  $\beta_G$  is now the derived parameter and is given by

$$\beta_G = \beta_{TG} \frac{C_{pG} + C_S(1 + j\omega\tau_{GS})^{-1}}{C_{vG} + C_S(1 + j\omega\tau_{GS})^{-1}} = P_0 \frac{C_{pG} + C_S(1 + j\omega\tau_{GS})^{-1}}{C_{vG} + C_S(1 + j\omega\tau_{GS})^{-1}} \quad (20)$$

The calculated relaxation times for all three gases are given in Figure 6 assuming a constant solid bulk modulus  $\beta_S$  of 400 kPa.

The calculated relaxation times are a function of several experimental variables and will be examined in depth in later reports. However, a few preliminary conclusions are apparent from the data. The first is that relaxation times increase with pressure in all of the gases examined, except for the lowest pressures near STP. Because of the increased experimental uncertainty in this range, we are reticent to attribute significance to the data collected at these low pressures. However, the increase in relaxation time through the rest of the experimental range can be attributed to a decreased fraction of collisions in the gas occurring with the pore wall. As pressure increases, the gas mean free path decreases and the time necessary for complete heat exchange increases.

The second conclusion lies in the anomalously high relaxation time of helium in the intermediate pressure range. As the lightest of the three gases, helium is expected to have the lowest accommodation coefficient of the three gases [24]. Subsequently, although the number of collisions between helium and the pore wall may be the highest, the amount of heat exchanged per collision is expected to be the lowest. A similarly drawn conclusion with regard to argon and nitrogen may be complicated by the contribution of diatomic nitrogen’s internal states to heat capacity and heat exchange.

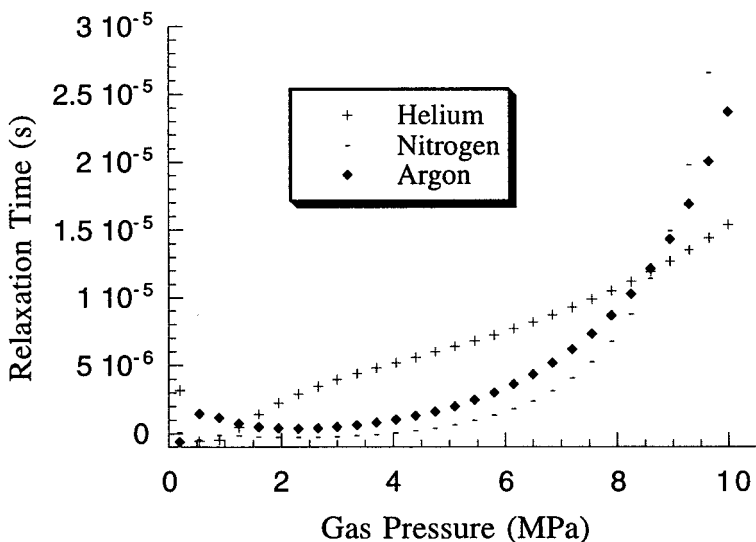


**Figure 6.** Derived relaxation time for all three gases as a function of pressure. A curve fit of the experimental data given in Figure 4 was used.

The use of acoustics for probing the solid microstructure of highly porous media and the dynamics of solid/gas interactions is limited primarily by the empirical realities of acoustic transduction and the range of materials which can be examined. The porous materials amenable to such examination must have densities and moduli which are comparable to the interstitial gas for acceptable signals and analysis. The high uncertainty at the lowest pressures in this examination bear witness to this fact. Air-coupled acoustic transducers are a relatively new technology, and further developments in technology will address this issue. Additionally, the unique chemical composition and microstructure aerogels may make it difficult to extrapolate into more common bulk materials.

## CONCLUSIONS

Acoustic propagation in the gaseous component of aerogels displays a combined adiabatic and isothermal nature that is a consequence of the microscale thermalization of the gas with the solid. Acoustic transmission through the aerogel creates a temperature difference between the gaseous and the solid component phases. The thermalization of these temperature differences is a microscopic process that influences the bulk acoustic propagation in the aerogel.

Acoustic velocity measurements in different gases at pressures up to 10 MPa display the loss of acoustic energy by the gaseous component. A theoretical description of the heat exchange yields a complex heat capacity and bulk modulus of the gas, and allows for the calculation of an empirical relaxation time.

The ultimate aim of this research is to relate these empirical relaxation times to the interaction between the interstitial gas and the solid aerogel through a consideration of the gas dynamics and heat exchange within individual pores. The current relaxation times are complex functions of several experimental variables. Further theoretical and experimental work is necessary to elucidate the significance of the various interactions that contribute to the empirical relaxation time.

## REFERENCES

1. P. P. Narang, A Theoretical Study of Sound Transmission through Aerogel Glazing Systems, *Appl. Acoust.*, vol. 34, pp. 249–259, 1991.
2. J. Gross, G. Reichenauer, and J. Fricke, Mechanical Properties of SiO<sub>2</sub> Aerogels, *J. Phys. D: Appl. Phys.*, vol. 21, pp. 1447–1451, 1988.
3. J. Gross, J. Fricke, and L. W. Hrubesh, Sound Propagation in SiO<sub>2</sub> Aerogels, *J. Acoust. Soc. Am.*, vol. 91, pp. 2004–2006, 1992.
4. A. Zimmerman, J. Gross, and J. Fricke, Constant-Q Acoustic Attenuation in Silica Aerogels, *J. Non-Cryst. Solids*, vol. 186, pp. 238–243, 1995.
5. H. Altmann, T. Schlieff, J. Gross, and J. Fricke, Ultrasonic Measurements on Silica and Organic Aerogels, *Ultrasonics Int. 91 Conf. Proc.*, pp. 261–265, 1991.
6. V. Gibiat, O. Lefevre, T. Woigner, J. Pelous, and J. Phalippou, Acoustic Properties and Potential Applications of Silica Aerogels, *J. Non-Cryst. Sol.*, vol. 186, pp. 244–255, 1995.
7. A. B. Wood, *A Textbook of Sound*, G. Bell and Sons, London, 1941.
8. G. Shumway, Sound Velocity vs. Temperature in Water-Saturated Sediments, *Geophysics*, vol. 23, pp. 494–505, 1958.



9. M. R. J. Wyllie, A. R. Gregory, and L. W. Gardner, Elastic Wave Velocities in Heterogeneous and Porous Media, *Geophysics*, vol. 21, pp. 41–70, 1956.
10. M. A. Biot, Theory of Propagation of Acoustic Waves in a Fluid-Saturated Porous Solid. I. Low-Frequency Range, *J. Acoust. Soc. Am.*, vol. 28, pp. 168–178, 1956.
11. M. A. Biot, Theory of Propagation of Acoustic Waves in a Fluid-Saturated Porous Solid. II. Higher Frequency Range, *J. Acoust. Soc. Am.*, vol. 28, pp. 179–191, 1956.
12. D. L. Johnson, J. Koplik, and R. Dashen, Theory of the Dynamic Permeability and Toruosity in Fluid-Saturated Media, *J. Fluid. Mech.*, vol. 176, pp. 379–402, 1987.
13. S. Q. Zeng, A. Hunt, and R. Greif, Mean Free Path and Apparent Thermal Conductivity of a Gas in a Porous Medium, *J. Heat Transfer*, vol. 177, pp. 758–761, 1995.
14. B. Hosticka, P. M. Norris, J. S. Brenizer, and C. E. Daitch, Gas Flow through Aerogels, *J. Non-Cryst. Solids*, vol. 225, pp. 293–297, 1998.
15. K. F. Herzfeld and T. A. Litovitz, *Absorption and Dispersion of Ultrasonic Waves*, pp. 55–66, 206–209, Academic Press, New York, 1959.
16. H. D. Gesser and P. C. Goswami, Aerogels and Related Porous Materials, *Chem. Rev.*, vol. 89, pp. 765–788, 1989.
17. C. Kittel and H. Kroemer, *Thermal Physics*, pp. 432–435, Freeman, New York, 1980.
18. G. Kirchhoff, Ueber den Einfluss der Waermeleitung in einem Gase auf die Schallbewegung, *Ann. Phys. Chem.*, vol. 6, pp. 177–193, 1868.
19. R. M. Logan and R. E. Stickney, Simple Classical Model for the Scattering of Gas Atoms From a Solid Surface, *J. Chem. Phys.*, vol. 44, pp. 195–201, 1966.
20. R. M. Logan and J. C. Keck, Classical Theory for the Interaction of Gas Atoms with Solid Surfaces, *J. Chem. Phys.*, vol. 49, pp. 860–876, 1968.
21. B. McCarroll and G. Ehrlich, Trapping and Energy Transfer in Atomic Collisions with a Crystal Surface, *J. Chem. Phys.*, vol. 38, pp. 523–532, 1963.
22. F. C. Hurlbut, Studies of Molecular Scattering at the Solid Surface, *J. Appl. Phys.*, vol. 28, pp. 844–850, 1957.
23. J. F. T. Conroy, B. Hosticka, S. C. Davis, and P. M. Norris, Evaluation of the Acoustic Properties of Silica Aerogels, *Proc. 1998 IMECE Conf., Porous, Cellular, and Microcellular Materials*, MD-Vol. 82, pp. 25–28, 1998.
24. Y. Song and M. M. Yovanovich, Contact Interface Gas Heat Transfer: A Method of Measuring Thermal Accommodation Coefficients, *Proc. Ninth Annual Int. Electronics Packaging Conf.*, San Diego, CA, pp. 925–936, 1989.